축소관 영역에서의 축대칭 액적 변형 거동의 유한요소해석 1. 비-뉴톤 유체

김시조, 한창대*

안동대학교 기계공학부
*애크론대학교 고분자공학과

Finite Element Analysis of Axisymmetric Motion of a Deformable Droplet in the Entrance Region of a Cylindrical Tube. 1.Non-Newtonian Fluids

See Jo Kim and Chang Dae Han*
School of Mechanical Engineering, Andong National University
Andong, Kyungbuk 760-749, Korea
*Department of Polymer Engineering, The University of Akron
Akron, Ohio 44325-0301

INTRODUCTION

In the 1970s Han and co-workers[1-3] conducted extensive measurements of pressure drops of dispersed two-phase polymer blends in the fully developed region of a cylindrical tube or a slit die and then calculated apparent (or bulk) rheological properties. They demonstrated that the bulk rheological properties of two-phase polymer blends depended very much on the blend morphology. It is not difficult to imagine that the bulk rheological properties of dispersed two-phase polymer blends would depend on the sizes and shapes of droplets. Since the droplets, when in motion, disturb the motion of the continuous phase, one can easily surmise that prediction of pressure drop (thus bulk rheological properties) of a dispersed two-phase polymer blend in a flow channel requires information on the shapes of droplets, which in turn are affected by the stresses in the flow field.

Very recently we have developed FEM computer codes to calculate the shape of a non-Newtonian droplet, suspended in another non-Newtonian liquid, moving along the central axis of a cylindrical tube including the entrance region. Specifically, using FEM together with an unstructured mesh generator and an auto-remeshing technique we solved a system of nonlinear equations describing the axisymmetric motion of a single non-Newtonian droplet suspended in another non-Newtonian liquid in the entrance region of a cylindrical tube. In this paper we present the highlights of our study, namely, the shape of a droplet as affected by the ratio of viscosities of the droplet and suspending medium, the capillary number, and the ratio of radii of the droplet and tube. For the computation, we first compare the computed shapes of droplet with the experimental results of Chin and Han[4,5] for three cases: (i) a droplet of 2 wt % solution of polyisobutylene

(PIB) in decalin suspended in 2 wt % aqueous solution of polyacrylamide (Separan, Dow Chemical Company), (ii) a droplet of 6 wt % PIB in decalin suspended in 2 wt % aqueous solution of Separan, and (iii) a droplet of 10 wt % PIB in decalin suspended in 2 wt % aqueous solution of Separan. And then, we investigate the effects of the undeformed droplet radius, shear rate of bulk fluid, and viscosity ratio of the droplet phase to the suspending medium on droplet shape.

FORMULATION AND NUMERICAL ALGORITHMS

In formulating finite element equations we used the principle of virtual power, which enabled us to include unsteady-state term in the momentum equation, and we applied the penalty function method, which simplified the system equations by eliminating the term containing pressure, thereby considerably reducing the computational time required. At each time step during numerical computations the stiffness matrices, forcing vectors, particle positions, and velocity were updated until the Lagrangian specification was met. At the early stage of computation, it was not necessary to use a remeshing procedure. For large deformations of finite elements, an auto-remeshing procedure was used to generate finer meshes around the interfaces of a droplet. We employed a two-dimensional unstructured mesh generator to deal with the moving boundary problems, where the shape of a droplet changes continuously while moving in the entrance region of a cylindrical tube. Automatic remeshing was found to be necessary during time marching, because a droplet placed at the upstream end of the reservoir section deformed continuously when approaching the tube entrance and while passing the entrance region until fully developed flow was achieved at the downstream end of the tube.

NUMERICAL RESULTS AND DISCUSSION

Figure 1 shows experimentally observed droplet shapes in the entrance region of a cylindrical tube having the reservoir radius of 5.35 cm, the tube radius of 0.3 cm, and the entrance angle of 30 degrees (see Figures 3a-3c in a paper of Chin and Han[5]): (a) a droplet of 2 wt % PIB solution suspended in a 2 wt % Separan solution with the undeformed droplet radius (r) of 0.12 cm and the shear rate of 75.4 (1/s), (b) a droplet of 6 wt % PIB solution suspended in a 2 wt % Separan solution with r = 0.091 cm and shear rate of 102.4 (1/s), (c) a droplet of 10 wt % PIB solution suspended by a 2 wt % Separan solution with r = 0.12 cm and shear rate of 102.4 (1/s).

Figure 2 gives the computed shapes of a 2 wt % PIB droplet of 1.2 mm in radius, suspended in 2 wt % Separan solution at shear rate=75.4(1/s), as it moves along the centerline of the conical reservoir section into the cylindrical tube, simulating the experimental results given in Figure 1a. It is seen that the droplet deforms considerably at the inlet of the tube and then recoils somewhat after entering the tube. It suffices to state that the computed droplet shape in the entrance region shows what is expected intuitively and also in reasonable agreement with experiment. Figure 3 gives the computed shapes of a 6 wt % PIB droplet of 0.9 mm in radius, suspended in 2 wt % Separan solution at shear rate=102.4(1/s), as it moves along the centerline of the conical reservoir section into the cylindrical tube, simulating the experimental results given in Figure 1b. Figure 4 gives the computed shapes of a 10 wt % PIB droplet of 1.2 mm in radius, suspended in 2 wt % Separan solution at shear rate=102.4(1/s), as it moves along the centerline of the conical reservoir section into the cylindrical tube, simulating the experimental results given in Figure 1c. In order to facilitate our discussion, enlarged droplet shapes at four different positions near and just inside the tube inlet are also given in Figures 2-4.

It is gratifying to observe that the computational results presented in Figures 2-4 are in general agreement with the experimental results given in Figure 1, giving us a confidence in the formulations and the numerical algorithms developed in this study(see the paper[6] for more details).

CONCLUSIONS

Finite element method (FEM) was employed to analyze axisymmetric motion of a deformable droplet in the entrance region of a cylindrical tube. In the present study a non-Newtonian droplet suspended in a non-Newtonian medium was considered, for which a truncated power-law model was employed. The penalty function method was used to eliminate the pressure variables from the system equations, considerably reducing the computational time required. In solving the system equations an in-house unstructured mesh generator and also an auto-remeshing technique were employed, which were necessary in order to describe the shape of a highly deformed droplet in the entrance region of a cylindrical tube. The FEM has simulated successfully the experimental results of Chin and Han (1979, 1980), describing the deformation of a droplet as it approaches the inlet of a cylindrical tube from the reservoir section and the recoil of the droplet after it enters the tube section. The present study has demonstrated the effects of the viscosity ratio of droplet to suspending medium and capillary number on the deformation of non-Newtonian droplets in the entrance region of a cylindrical tube.

REFERENCES

1. Han, C. D. and K. Funatsu, *J. Rheol.* **22**, 113 (1978).
2. Han, C. D. and Y. W. Kim, *Trans. Soc. Rheol.* **19**, 245 (1975).
3. Han, C. D., Y. W. Kim and S. J. Chen, *J. Appl. Polym. Sci.* **19**, 2831 (1975).
4. Chin, H. B. and C. D. Han, *J. Rheol.* **23**, 557 (1979).
5. Chin, H. and C. D. Han, *J. Rheol.* **24**, 1 (1980).
6. Kim, S. J. and C. D. Han, "Finite Element Analysis of Axisymmetric Motion of a Deformable Droplet in the Entrance Region of a Cylindrical Tube. 1. Non-Newtonian Fluids," Submitted to *J. Rheol.*

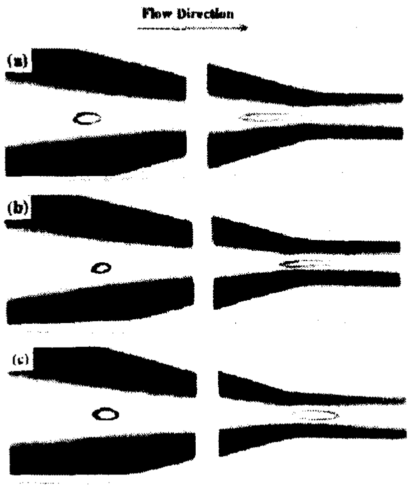

Fig. 1. Experimentally observed droplet shapes in a cylindrical tube (see Figures 3a-3c in a paper of Chin and Han, 1980).

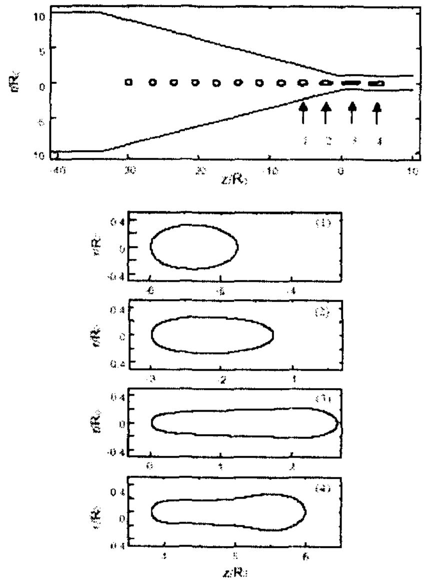

Fig. 2. Computed droplet shapes, simulating via FEM the experimental result given in Figure 1a.

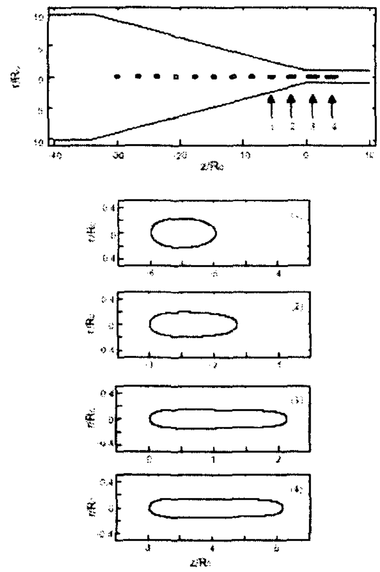

Fig. 3. Computed droplet shapes, simulating via FEM the experimental result given in Figure 1b.

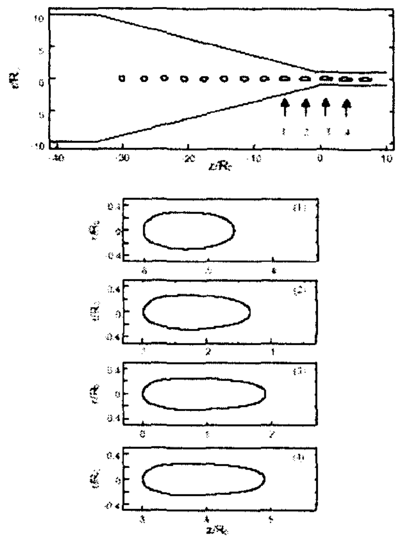

Fig. 4. Computed droplet shapes, simulating via FEM the experimental result given in Figure 1c.